Computational Research Progress in Applied Science & Engineering
©PEARL publication, 2016

ISSN 2423-4591

CRPASE Vol. 02(02), 55-64, April 2016

Dynamical Modeling and Control of Fully-actuated Stratospheric Airship

Behnam Miripour Fard*, Pegah Abdollahzadeh, Nima Noori

Department of Robotics Engineering, Hamedan University of Technology, 65155-579 Hamedan, Iran

Keywords

Stratospheric airship,
Fully-actuated,
Inverse dynamic control,
Uncertainties.

Abstract

This paper presents dynamic modeling and adaptive control of a stratospheric airship. In spite of many progresses, there are still fundamental challenges in this field of study. In the present paper, first the dynamic model of fully-actuated stratospheric airship with 6-DOF has expressed by the generalized coordinates. With consideration of uncertainties in inertial parameters, based on adaptive inverse dynamic control, first inertial parameters are estimated online by using linear parameterization and gradient update law. Later on by designing movement algorithm based on passivity, control law is deduced and adaptive and robust control methods based on passivity are applied for controlling of the airship. The stability of the closed loop control system is proved using the Lyapunov stability theory. Comparison between the Simulation results of the both methods in tracking of the desired time-dependent variable path is shown.

1. Introduction

Airships are light vehicles which the buoyant force makes them to float in the air, hence, they are large and they move slowly. Also, they possess flight controls and propulsion force supply motors.

As height from the ground increases, there is an atmospheric classification in which some parameters are of great importance.Troposphere is the lowest layer of atmosphere which is consisted of smaller layers. The difference between this layer and others is that the whole volume of water vapor of the Earth's atmosphere is contained in this layer. Accordingly, many of atmospheric phenomena that are related to moisture and crucial to weather condition (such as clouds, rain, snow, mist and thunder), take place in this layer. Thermal source of troposphere is the energy emitted from the ground; therefore, as altitude increases, the temperature decreases. Thickness of troposphere adheres to different thermal conditions in different geographical latitudes. This thickness ranges from 17 km to 18 km in the equator and 10 km to 11 km in temperate regions and 7 km to 8 km in the poles.

The stratosphere is above the troposphere and its mean thickness is about 23 km. In its first 3 km, the temperature is constant but at higher parts the temperature increases as altitude rises. In stratosphere clouds do not form very often. This layer is the safest layer of the atmosphere and has the most proper weather condition for airship to function. In this layer wind moves slowly; hence, many scientists have tried so much to develop airships to operate in this layer. In this height from the ground, airships have more advantageous than other aerial objects and satellites in doing scientific researches, online monitoring, carrying load, etc.

Controlling airships in stratosphere is an issue that has vital importance in the development of these vehicles. In the study of control of airships, control methods such as PID for controlling longitudinal velocity and PD for controlling altitude and orientation of airships have been used [1]. The linear control theory for stability control of airships in [2] and feedback control in [3] have been studied. In fact, these methods are viable exclusively to linearized model of the airship and around the equilibrium point. The inverse dynamic for autonomous airships are utilized based on non-linear model [4]. When implementing this method, it is essential to have feed-forward acceleration and the inertia matrix reversible. To have a breakthrough in facing these two issues, dynamic control is introduced based on passivity. These techniques are solely for fully-actuated airships. This means that the stability of closed-loop system is not guaranteed for under-actuated airships [5, 6].

Although there are many advanced control schemes like sliding mode control [7], optimal control [8], model predictive control [9] and etc. that can be implemented on the airship model, but because of the special dynamic behavior of the airship, adaptive and robust control methods

* Corresponding Author:
E-mail address: bmf@hut.ac.ir– Tel, +98 (81) 38411526 – Fax, +98 (81) 38411520

Received: 25 December 2015; Accepted: 21 March 2016

based on passivity are used in this paper for fully-actuated dynamic model with 6-DOF and with flight controls of rudders and elevators and actuators which are fixed under the airbone.

2. Airship Model

The simulated model of this study is shown in Figure 1.

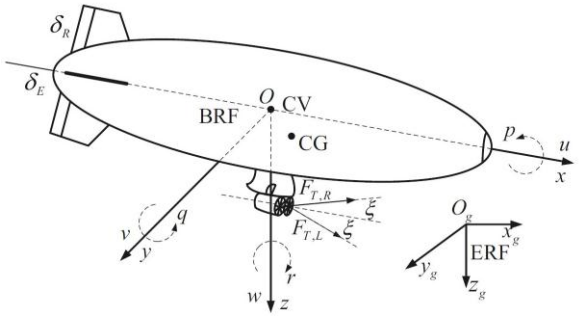

Figure 1. Model of stratospheric airship

As it is shown in Figure 1, the model of the airship has an elliptical volume. Moreover, the airship's buoyant force is produced by helium. Dynamic flight controls such as elevators and rudders are attached to its flight tail. It is assumed that both upper and lower rudders move simultaneously; also, both left and right elevators move together. The effects of these deviations are defined as $u_g \triangleq \{\delta_{RUD}\ , \delta_{ELV}\}$ and the vector of control forces provided by motors is u_F. Control input is defined as $u = [u_F\ , u_\delta]^T$ and is expressed by relation (1).

$$u = \left[F_{T,L}c\mu_l, F_{T,R}c\mu_R, F_{T,L}s\mu_l, F_{T,R}s\mu_R, \delta_{ELVL}\ , \delta_{ELVR}\right]^T \qquad (1)$$

where$F_{T,L}$ and $F_{T,R}$ are motor forces and μ_L and μ_R are rotational angles of left and right impellers with respect to y-axis of the frame attached to the body.

As shown in Figure 1, the inertia frame with its origin O_g is placed on a fixed point on the ground. The axis $O_g x_g$ is pointed toward north and the axis $O_g z_g$ is toward the core of the Earth and the axis $O_g y_g$ is toward east. The frame attached to body with its origin O is fixed on the center of volume of the airship. The axis O_x is toward the nose and the axis O_z is perpendicular to the former and toward down-side and the axis O_y can be discovered using right hand rule. The position and orientation of the airship are indicated by $\zeta = \left[x_g, y_g, z_g\right]^T$ and Euler angles $\gamma = [\varphi, \theta, \psi]^T$ in inertia frame, respectively. Moreover, the linear and angular velocities of the airship are defined by $v = [u, v, w]^T$ and $\omega = [p, q, r]^T$ in the frame attached to the body, respectively. Since the structure of the airship around the transversal plane is symmetrical, the *y* coordinate of center of mass and the inertia products are $y_{cg} = 0$and $\{I_{xy}, I_{yz}\} = 0$, respectively.

$$\bar{A} = \begin{bmatrix} I_x & 0 & -I_{xz} & 0 & -mz_{cg} & 0 \\ 0 & I_y + \rho\nabla k_3 & 0 & mz_{cg} & 0 & -mx_{cg} \\ -I_{xz} & 0 & I_z + \rho\nabla k_3 & 0 & mx_{cg} & 0 \\ 0 & mz_{cg} & 0 & m + \rho\nabla k_1 & 0 & 0 \\ -mz_{cg} & 0 & mx_{cg} & 0 & m + \rho\nabla k_2 & 0 \\ 0 & -mx_{cg} & 0 & 0 & 0 & m + \rho\nabla k_2 \end{bmatrix}$$

$$\bar{N} = \begin{bmatrix} -(I_z - I_y)qr + I_{xz}pq + mz_{cg}(ur - wp) + L_a \\ -(I_x - I_y - \rho\nabla k_3)pr - I_{xz}(p^2 - r^2) - mz_{cg}(wp - vr) + mx_{cg}(vp - uq) + M_a \\ -(I_y + \rho\nabla k_3 - I_x)pq - I_{xz}qr - mx_{cg}(ur - wp) + N_a \\ -(m + \rho\nabla k_2)(wp - vr) - mz_{cg}pr + mx_{cg}(q^2 + r^2) + X_a \\ (m + \rho\nabla k_2)wp - (m + \rho\nabla k_1)ur - mx_{cg}pq - mz_{cg}qr + Y_a \\ (m + \rho\nabla k_1)uq - (m + \rho\nabla k_2)vp - mx_{cg}rp + mx_{cg}(p^2 + q^2) + Z_a \end{bmatrix}$$

In the above expressions, m, ∇, $\{x_{cg}, z_{cg}\}$, $\{k_1, k_2, k_3\}$, ξ, $\{x_p, y_p, z_p\}$ and $\{x_p, -y_p, z_p\}$ are the mass of the airship, volume of the airship's airbone, the coordinates of the center of mass (CG), inertia coefficient of ellipse for calculating the extra mass and the inertia matrix, the open angle of left and right impellers, position of right motor and

When modeling airships, generally, there are some assumptions made to ease the process. Similar to [11], these assumptions in this paper are as following

- Airship's body has a solid structure, so it is possible to neglect the aero-elastic effects.
- The center of mass and the center of buoyancy are coincided with.
- Because of minor effect of Roll angle, the movement is considered horizontally and taking place in the xy-plane.

The kinematic equation of the position is defined by Eq. (2) as below

$$\dot{\zeta} = \begin{bmatrix} c\theta c\psi & s\theta c\psi s\varphi - s\psi c\varphi & s\theta c\psi c\varphi + s\psi s\varphi \\ c\theta s\psi & s\theta c\psi s\varphi + c\psi c\varphi & s\theta c\psi c\varphi - c\psi s\varphi \\ -s\theta & c\theta s\varphi & c\theta c\varphi \end{bmatrix} \begin{bmatrix} u \\ v \\ w \end{bmatrix} \triangleq R_b(\gamma)v \qquad (2)$$

The kinematic equation of orientation is defined by Eq. (3) as

$$\dot{\gamma} = \begin{bmatrix} 1 & t\theta s\varphi & t\theta c\varphi \\ 0 & c\varphi & -s\varphi \\ 0 & s\varphi/c\theta & c\varphi/c\theta \end{bmatrix} \begin{bmatrix} u \\ v \\ w \end{bmatrix} \triangleq R_\gamma(\gamma)\omega \qquad (3)$$

Finally, the dynamic equation of movement is defined by Eq. (4) as

$$\bar{A}\begin{bmatrix} \dot{\omega} \\ \dot{v} \end{bmatrix} = \bar{N} + \bar{G} + \bar{B}\begin{bmatrix} \mathrm{u}_F \\ \mathrm{u}_\delta \end{bmatrix} \qquad (4)$$

where

$$\bar{G} = \begin{bmatrix} -z_{cg}mg\cos\theta\sin\varphi \\ -z_{cg}mg\sin\theta - x_{cg}mg\cos\theta\cos\varphi \\ x_{cg}mg\cos\theta\sin\varphi \\ (B_g - mg)\sin\theta \\ -(B_g - mg)\cos\theta\sin\varphi \\ -(B_g - mg)\cos\theta\cos\varphi \end{bmatrix},$$

$$\bar{B} = \begin{bmatrix} cos\xi & \cos\xi & 0 & 0 & 0 & 0 \\ \sin\xi & -\sin\xi & 0 & 0 & 0 & -2QC_{M4} \\ 0 & 0 & 1 & 1 & -2QC_{N4} & 0 \\ -zp\sin\xi & -zp\sin\xi & yp & yp & 0 & 0 \\ zp\cos\xi & zp\cos\xi & -xp & -xp & -2QC_{Y4} & 0 \\ xp\sin\xi - yp\cos\xi & xp\sin\xi + yp\cos\xi & 0 & 0 & 0 & -2QC_{Z4} \end{bmatrix}$$

position of left motor in the frame fastened to the trunk, respectively. Then, we have $B_g \equiv mg$, where g is the gravity acceleration and B_g is the buoyant force and is applied to the center of volume of the airship. $Q = \rho U^2/2$ is the dynamic pressure, where ρ is the density of atmosphere in the flight altitude and $U = \sqrt{u^2 + v^2 + w^2}$ is the velocity of the airship. $C_{i4}(i = L, M, N, Y, Z)$ are the aerodynamic coefficients which are explained in details in [14]. Eventually, $\{X_a, Y_a, Z_a\}$ and $\{L_a, M_a, N_a\}$ are the aerodynamic forces and torques in the frame attached to the body, respectively, and are described in the appendix.

By choosing the generalized coordinates (5) and considering kinematic Eqs. (2) and (3), Eq. (6) which indicates the linear and angular velocities of the airship, is obtained. It is assumed that γ satisfies the conditions $|\varphi| < \pi$ and $|\theta| < \pi/2$ for $R_\gamma(\gamma)$ to be reversible, permanently [4].

$$\mu = [\varphi, \theta, \psi, x_g, y_g, z_g]^T \tag{5}$$

$$V = \begin{bmatrix} S_1 & O_3 \\ O_3 & S_2 \end{bmatrix} \dot{\mu} \triangleq S\dot{\mu} \tag{6}$$

where

$$S_1 = \begin{bmatrix} 1 & 0 & -s\theta \\ 0 & c\varphi & -s\varphi s\theta \\ 0 & -s\varphi & c\varphi c\theta \end{bmatrix}$$

$$S_2 = \begin{bmatrix} c\theta c\psi & c\theta s\psi & -s\theta \\ s\theta c\psi s\varphi - s\psi c\varphi & s\theta c\psi s\varphi + c\psi c\varphi & c\theta s\varphi \\ s\theta c\psi c\varphi + s\psi s\varphi & s\theta c\psi c\varphi - c\psi s\varphi & c\theta c\varphi \end{bmatrix}$$

Eq. (7) is derived by getting differentiation from Eq. (6). Then, by multiplying $\bar{A}$ to the both sides of Eq. (7), Eq. (8) is obtained.

$$\dot{V} = \dot{S}\dot{\mu} + S\ddot{\mu} \tag{7}$$

$$\bar{A}\dot{V} = \bar{A}\dot{S}\dot{\mu} + \bar{A}S\ddot{\mu} \tag{8}$$

The matrix $\dot{S}$ is obtained according to Eq. (9) and by using skew-symmetric matrix $s(\omega(t))$.

$$s(\omega(t)) = \begin{bmatrix} 0 & -r & q \\ r & 0 & -p \\ -q & p & 0 \end{bmatrix} \tag{9}$$

Using Eqs. (4) and (6), movement equation, according to generalized coordinates, is obtained as below

$$A(\mu)\ddot{\mu} + N(\mu, \dot{\mu})\dot{\mu} + G(\mu) = B(\mu)u \tag{10}$$

where $B(\mu) = \bar{B}$, $G(\mu) = -\bar{N} - \bar{G}$, $N(\mu, \dot{\mu}) = \bar{A}\dot{S}$ and $A(\mu) = \bar{A}S$. Both A and S are reversible and $\bar{A}$ is positive definition; hence, A is reversible and positive definition, too. Similarly, as $|B(\mu)| \neq 0$, $B(\mu)$ is reversible, too.

Considering $\tau = B(\mu)u$, Eq. (10) can be rewritten in the following form

$$A(\mu)\ddot{\mu} + N(\mu, \dot{\mu})\dot{\mu} + G(\mu) = \tau \tag{11}$$

The reverse of model in controlling systems with non-linear dynamic is a momentous issue, for derivatives of system model's signals are acquired from current and next states. The exact derivative of the model needs system's next states, which is not possible. accordingly, we use an approximating method named quasi-derivatives.

In general, there are two types of quasi-derivative; one from first order and the other one from second order. Here, as in [11], the second order quasi-derivatives are used in accordance with Eq. (12) as

$$\begin{aligned} \dot{x}_1(t) &= x_2(t) \\ \dot{x}_2(t) &= -{\omega_d}^2\big(x_1(t) - \delta(t)\big) - 2\xi_d\omega_d x_2(t) \\ \sigma(t) &= x_2(t) \end{aligned} \tag{12}$$

where $\sigma(t)$ is $\delta(t)$'s quasi-derivative. $\xi_d$equals to constant amount of 0.707 and is considered as the optimized attenuation coefficient. $\omega_d$is the bandwidth that as it gets larger the approximation, which here is considered as 0.5, becomes better.

3. Calculation of Desired Values

In each moment t, tangent to ζ_c is equal to $\dot{\zeta}_c = [\dot{x}_c, \dot{y}_c, \dot{z}_c]$. θ_c, which obtains using Eq. (13), is the angle between $\dot{\zeta}_c$ and the $O_g x_g y_g$ plane in the inertia frame. Also, ψ_c is the angle between the projection of $\dot{\zeta}_c$ on the $O_g x_g y_g$ plane and $O_g x_g$ axis. So

$$\theta_c = \arctan2\big(-\dot{z}_c, \sqrt{\dot{x}_c + \dot{y}_c}\big) \tag{13}$$

$$\psi_c = \arctan2(\dot{y}_c, \dot{x}_c) \tag{14}$$

The linear velocities of the airship acquires from position's kinematic Eq. (2), in accordance with Eq. (15) as

$$v_c = R_b^{-1}(\gamma_c)\dot{\zeta}_c \tag{15}$$

where $\dot{\zeta}_c$ is obtained from ζ_c and quasi-derivatives of Eq. (12). The angular velocities are acheived from orientation's kinematic, Eq. (3), in according to the following relation

$$\omega_c = R_\gamma^{-1}(\gamma_c)\dot{\gamma}_c \tag{16}$$

in which $\dot{\gamma}_c$ gets from γ_c and quasi-derivatives of Eq. (12).

4. Control

In this section, the adaptive inverse dynamic scheme is described. By considering the inertia parameters vector $\eta = [I_x, I_y, I_z, I_{xz}, mz_{cg}]^T$ and the inertia parameters vector $\hat{\eta} = [\hat{I}_x, \hat{I}_y, \hat{I}_z, \hat{I}_{xz}, m\hat{z}_{cg}]^T$, as an approximation of η, the non-linear feedback control law is obtained as

$$u = B^{-1}(\mu)\big[\hat{A}(\mu)a_x + \hat{N}(\mu, \dot{\mu})\mu + \hat{G}(\mu)\big] \tag{17}$$

where $\hat{G}$, $\hat{N}$ and $\hat{A}$ in terms η are approximations of G, N and A, respectively. By substituting Eq. (17) into Eq. (16) and then substituting Eq. (18) in it and using linear parameterization, Eq. (19) is achieved.

$$a_x = \ddot{\mu}^d - K_0(\mu - \mu^d) - K_1(\dot{\mu} - \dot{\mu}^d) \tag{18}$$

$$\ddot{\tilde{\mu}} + K_1\dot{\tilde{\mu}} + K_0\tilde{\mu} = \hat{A}(\mu)^{-1}Y(\mu, \dot{\mu}, \ddot{\mu})\tilde{\eta} \tag{19}$$

where Y is the regressor matrix. Eq. (19) transforms into (20) in state space.

$$\dot{e} = Ae + B\boldsymbol{\Phi}\tilde{\eta} \tag{20}$$

where

$$A = \begin{bmatrix} O_6 & I_6 \\ -K_0 & -K_1 \end{bmatrix}, B = \begin{bmatrix} O_6 \\ I_6 \end{bmatrix}, \Phi = \hat{A}(\mu)^{-1} Y(\mu, \dot{\mu}, \ddot{\mu})$$

Also, K_0 and K_1 are diagonal matrices. Assuming that P is a positive definition unique symmetric matrix that satisfies Lyapunov Eq. (21), parameter update law is chosen as Eq. (22) [6].

$$A^T P + PA = -Q \tag{21}$$

$$\dot{\hat{\eta}} = -\Gamma^{-1}\boldsymbol{\Phi}^T B^T P e \tag{22}$$

4.1. Control Based on Passivity

In this section, as opposed to adaptive inverse dynamic method, the system remains non-linear and the control law is chosen as expression (23).

$$\tau = A(\mu)a + N(\mu, \dot{\mu})v + G(\mu) + K_d r \tag{23}$$

where

$$\mathrm{e} = \mu_\mathrm{d} - \mu$$

$$v = \dot{\mu}_\mathrm{r} = \mu_\mathrm{d} + \Lambda(\mu_d - \mu) = \dot{\mu}_d + \Lambda e$$

$$\mathrm{a} = \dot{\mathrm{v}} = \ddot{\mu}_\mathrm{r} = \ddot{\mu}_\mathrm{d} + \Lambda(\dot{\mu}_\mathrm{d} - \dot{\mu}) = \ddot{\mu}_\mathrm{d} + \Lambda\dot{\mathrm{e}}$$

$$\mathrm{r} = \mathrm{v} - \dot{\mu} = \dot{\mu}_\mathrm{r} - \dot{\mu}$$

Here, K_d and Λ are constant positive definition diagonal matrices. To avoid convoluted calculations, S^T is multiplied to the left side of matrices A, N, G and B and the control law is expressed in (24a) and (24b).

$$\tau = \mathrm{A}(\mu)\ddot{\mu}_\mathrm{r} + \mathrm{N}(\mu, \dot{\mu})\dot{\mu}_\mathrm{r} + \mathrm{G}(\mu) + S^{-T}\mathrm{K_d}(\dot{\mu}_\mathrm{r} - \dot{\mu}) \tag{24a}$$

$$u = B^{-1}(\mu)[\mathrm{A}(\mu)\ddot{\mu}_r + \mathrm{N}(\mu, \dot{\mu})\dot{\mu}_\mathrm{r} + \mathrm{G}(\mu) + S^{-T}\mathrm{K_d}(\dot{\mu}_\mathrm{r} - \dot{\mu}) \tag{24b}$$

By equalizing Eqs. (16) and (24), Eq. (25), which is still a coupled non-linear system, will be resulted as

$$\mathrm{A}(\mu)\dot{\mathrm{r}} + \mathrm{N}(\mu, \dot{\mu})\mathrm{r} + \mathrm{G}(\mu) + \mathrm{S}^{-\mathrm{T}}\mathrm{K_d}\mathrm{r} = 0 \tag{25}$$

4.2. Designing Adaptive Control Law Based on Passivity

In this section, as before, by assuming uncertainties in inertia parameters, the control law can be defined by Eqs. (26a) and (26b) as

$$\tau = \hat{A}(\mu)\ddot{\mu}_r + \hat{N}(\mu, \dot{\mu})\dot{\mu}_\mathrm{r} + \hat{\mathrm{G}}(\mu) + S^{-T}\mathrm{K_d}(\dot{\mu}_\mathrm{r} - \dot{\mu}) \tag{26a}$$

$$u = B^{-1}(\mu)[\hat{A}(\mu)\ddot{\mu}_r + \hat{N}(\mu, \dot{\mu})\dot{\mu}_\mathrm{r} + \hat{G}(\mu) + S^{-T}\mathrm{K_d}(\dot{\mu}_\mathrm{r} - \dot{\mu})] \tag{26b}$$

Substituting Eq. (26) into Eq. (11), the following relation (27) is obtained as

$$\begin{aligned} &\mathrm{A}(\mu)\dot{\mathrm{r}} + \mathrm{N}(\mu, \dot{\mu})r + \mathrm{G}(\mu) + \mathrm{S}^{-\mathrm{T}}\mathrm{K_d}\mathrm{r} \\ &= \tilde{\mathrm{A}}(\mu, \eta - \hat{\eta})\ddot{\mu}_\mathrm{r} + \tilde{\mathrm{N}}\big(\mu, \eta - \hat{\mathrm{\eta}}\big)\dot{\mu}_\mathrm{r} + \tilde{\mathrm{G}}(\mu, \eta - \hat{\mathrm{\eta}}) \\ &= \hat{\mathrm{A}}(\mu, \ddot{\mu}_r, \tilde{\eta})\ddot{\mu}_r + \hat{\mathrm{N}}(\mu, \dot{\mu}, \dot{\mu}_r, \tilde{\eta})\dot{\mu}_r + \hat{\mathrm{G}}(\mu, \tilde{\eta}) \\ &= \left[\hat{\hat{\mathrm{A}}}(\mu, \ddot{\mu}_r) + \hat{\hat{\mathrm{N}}}(\mu, \dot{\mu}, \dot{\mu}_r) + \hat{\hat{\mathrm{G}}}(\mu)\right]\tilde{\eta} \\ &\triangleq \mathrm{Y}(\mu, \dot{\mu}, \dot{\mu}_r, \ddot{\mu}_r)\tilde{\eta} \end{aligned} \tag{27}$$

in which $\tilde{A} = A - \hat{A}$, $\tilde{N} = N - \hat{N}$, $\tilde{G} = G - \hat{G}$, $\tilde{\eta} = \eta - \hat{\eta}$, $\hat{\eta} \neq \eta$, $\tilde{A} \neq A$, $\tilde{N} \neq 0$ and $\tilde{G} \neq 0$. Thus, from dynamic Eq. (27) and by using five-dimension parametric space to approximate $\hat{\eta}$ and also using update gradient law, Eq. (28) is developed as

$$\dot{\hat{\eta}} = \Gamma^{-1} Y^T S r \tag{28}$$

where Γ is a positive definit matrix.

4.3. Designing Robust Control Law Based on Passivity

In the current section, akin to the previous section, by assuming uncertainties in inertia parameters, the control law is considered identical with Eqs. (26a) and (26b). The solitary contrast is that in this one we have $\hat{\eta}$ as below

$$\tilde{\eta} = \eta_0 + \delta\eta \tag{29}$$

where η_0 and $\delta\eta$ are nominal parameter vector and additional controlling term, respectively. By considering $\tilde{\eta} = \eta_0 - \eta$, which is a constant vector and indicates parametric uncertainty in system, Eq. (27) can be written in the following form

$$\mathrm{A}(\mu)\dot{\mathrm{r}} + \mathrm{N}(\mu, \dot{\mu})\mathrm{r} + \mathrm{G}(\mu) + \mathrm{S}^{-\mathrm{T}}\mathrm{K_d}\mathrm{r} = \mathrm{Y}(\mu, \dot{\mu}, \dot{\mu}_\mathrm{r}, \ddot{\mu}_\mathrm{r})(\tilde{\eta} + \delta\eta) \tag{30}$$

Considering the constant bound $\rho_i \geq 0$ separately for each inertia parameter as in Eq. (31), the control law of Eq. (32) can be achieved as

$$|\tilde{\eta}_i| \leq \rho_i, \quad i = 1, \ldots, 5 \tag{31}$$

$$\delta\eta = \begin{cases} -\rho_i \xi_i / |\xi_i| & \text{if } |\xi_i| > \varepsilon_\mathrm{i} \\ -\rho_i \xi_i / \varepsilon_\mathrm{i} & \text{if } |\xi_i| \leq \varepsilon_\mathrm{i} \end{cases} \tag{32}$$

where ξ_is indicate elements of matrix $Y^T r$ and ε_is are positive constants.

5. Stability Analysis

In the adaptive inverse dynamic by choosing the Lyapunov function as

$$L(t) = e^t Q e + \tilde{\theta}^T \Gamma \tilde{\theta} \tag{33}$$

Its derivative $\dot{L}(t)$ is calculated as below in accordance to Eq. (22)

$$\dot{L}(t) = e^t Q e + 2\tilde{\theta}^T \left\{\boldsymbol{\Phi}^T B^T P e + \Gamma\dot{\hat{\theta}}\right\} = -e^T Q e \tag{34}$$

It can be concluded from Eq. (34) that the tracking error converges to zero asymptotically and the error of approximating parameters remains bounded.

In the method of control based on passivity the candidate Lyapunov function will be chosen as (35).

The derivative of candidate function along the path of closed-loop system tallies Eq. (36) as

$$L(t) = \frac{1}{2}[r^T S^T \bar{A} S r + \tilde{\eta}^T \Gamma \tilde{\eta}] \quad (35)$$

$$\begin{aligned} \dot{L}(t) &= r^T S^T \dot{\bar{A}} S r + r^T S^T \bar{A} S \dot{r} + \tilde{\eta}^T \Gamma \dot{\tilde{\eta}} \\ &= r^T S^T (\dot{\bar{A}} S r + \bar{A} S \dot{r}) \\ &= r^T S^T (N r + A \dot{r}) + \tilde{\eta}^T \Gamma \dot{\tilde{\eta}} \\ &= r^T S^T (N r - N r - S^{-T} \mathrm{K_d} r + \mathrm{Y} \tilde{\eta}) + \tilde{\eta}^T \Gamma \dot{\tilde{\eta}} \\ &= -r^T \mathrm{K_d} r \le 0 \end{aligned} \quad (36)$$

It can be seen that $L(t)$ is bounded continually due to Eq. (36) and tracking the path asymptotically is guaranteed.

In the method of robust control based on passivity, by choosing candidate Lyapunov function of Eq. (37) and doing simple calculations $\dot{L}(t)$ will be acquired as

$$L(t) = \frac{1}{2}[r^T S^T \bar{A} S r + \tilde{\mu}^T \Lambda S^{-T} \mathrm{K_d} \tilde{\mu}] \quad (37)$$

$$\dot{L}(t) = -e^T Q e + r^T Y (\tilde{\eta} + \delta \eta) \quad (38)$$

By considering [13], it can be exposed that Lyapunov function satisfies the relation $\dot{L}(t) < 0$ for Eq. (39) as

$$\|e\| > \left(\frac{1}{\lambda_{min}(Q)} \sum_{i=1}^{p} \frac{\rho_i \varepsilon_i}{2} \right)^{1/2} \quad (39)$$

in which $\lambda_{min}(Q)$ is the minimum eigenvalue of Q.

6. Results and Discussion

The desired path for simulating trajectory tracking in an ascending spiral way is chosen as $\zeta_c = [500\sin(0.01t), 500\cos(0.01t), 0.1t + 20000]^T$. The direction of z-axis of the framed attached to the ground has been defined downward and is opposing to direction of height; consequently, $h = -z$ has been utilized instead of z. Therefore, we have $z_c = -h_c$.

Based on the alues of parameters and coefficients of the airship (Table 1), the situation and state of the system is expressed as

$\mu_0 = [0.1,0,0,0,550,20000]^T$, $V_0 = [0,0,0,4,0,0]^T$,
$\eta_0 = [3 \times 10^7, 2.5 \times 10^8, 2.5 \times 10^8, -2 \times 10^4, 2.8 \times 10^5]$,
$\varepsilon = [10^{-3}, 10^{-5}, 10^{-6}, 0.5 \times 10^{-4}, 0.5]$, $\Lambda = I_{6*6}$, $\Gamma = I_{6*6}$,
$\rho = [2 \times 10^7, 0.4 \times 10^8, 0.4 \times 10^8, 4 \times 10^4, 5.6 \times 10^5]$

The gains of the adaptive inverse dynamic method are defined as

$K_0 = diag\{2,3,2,1,1,1\}$, $K_1 = diag\{1,1,1,10,10,10\}$

The gain of the adaptive and robust control method based on passivity has been defined as below

$K_0 = diag\{10^8, 10^9, 10^8, 10^4, 10^5, 10^6\}$

According to the section 4 desired values of pitch and yaw can be calculated using the equations below

$\theta_c = \arctan2(0.1,5) = 0.02$
$\psi_c = \arctan2(-5 \times \sin(0.01 \times t), 5 \times \cos(0.01 \times t))$
$\varphi_c = 0$

The simulation results of orientation of the airship are shown in Figures 2 to 4.

Table 1. Values of parameters and coefficients of the airship

Parameters [5]	Values
m	$5.6 \times 10^4 (kg)$
∇	$7.4 \times 10^5 (m^3)$
ρ	$0.089\ (kgm^{-3})$
ξ	$\pi/6\ (rad)$
$\{x_{cg}, z_{cg}\}$	$\{0,15\}(m)$
I_x	$5 \times 10^7 (kgm^2)$
I_y	$2.9 \times 10^8 (kgm^2)$
I_z	$2.9 \times 10^8 (kgm^2)$
I_{xz}	$-6 \times 10^4 (kgm^2)$
k_1	0.105
k_2	0.825
k_3	0.52
C_{Y4}	-657
C_{Z4}	-657
C_{M4}	-7.7×10^4
C_{N4}	$-C_{M4}$

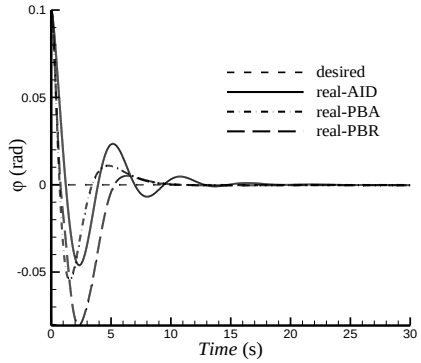

Figure 2. Roll angle

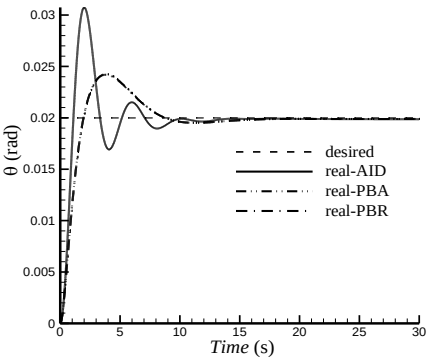

Figure 3. Pitch angle

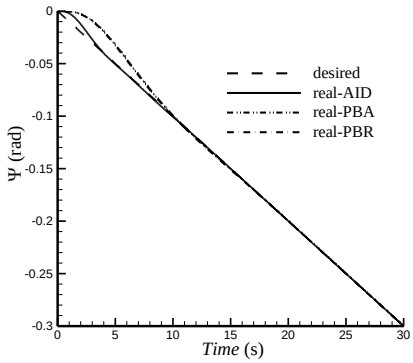

Figure 4. Yaw angle

Simulation results of the linear and angular velocities' error, trajectory tracking and motors' torques are expressed by Figures 5 to 13, respectively.

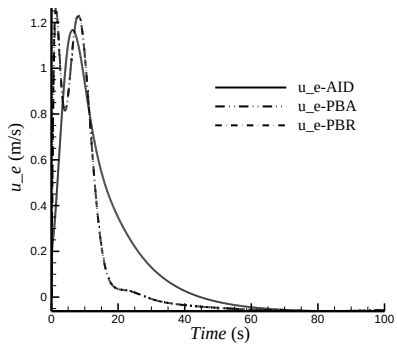

Figure 5. Error of linear velocity along *x*

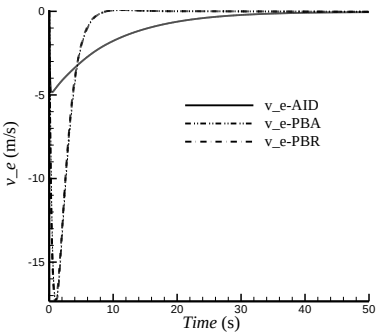

Figure 6. Error of linear velocity along y

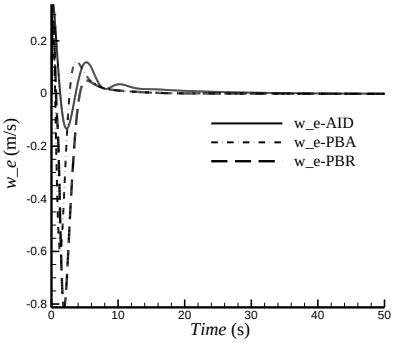

Figure 7. Error of linear velocity along *z*

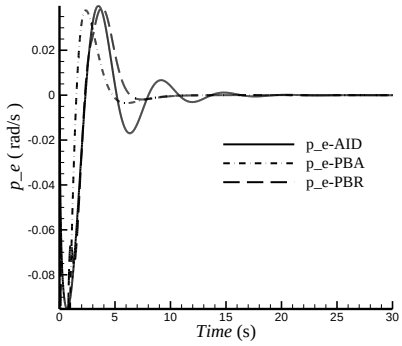

Figure 8. Error of angular velocity about *x*

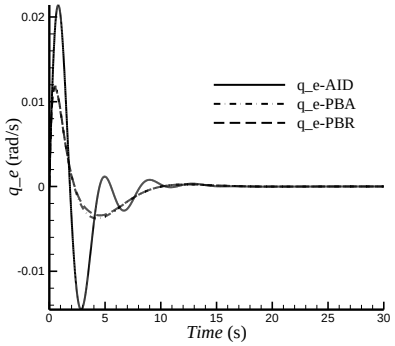

Figure 9. Error of angular velocity about *y*

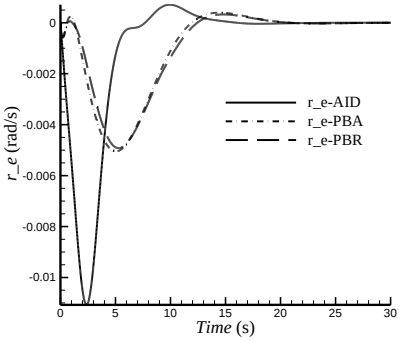

Figure 10. Error of angular velocity about *z*

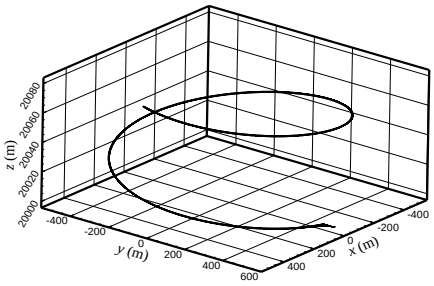

Figure 11. Trajectory tracking of stratospheric airship

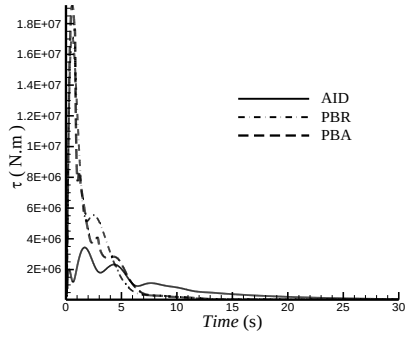

Figure 12. Torque of the left thrust

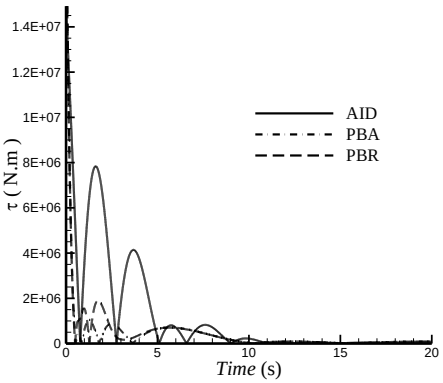

Figure 13. Torque of the right thrust

The results from simulation for estimating inertia parameters in adaptive control method based on passivity, adaptive inverse dynamic method and robust control method based on passivity are shown in Figures 14 to 18, 19 to 21 and 22 to 26, respectively.

As parameters' fluctuations in the first two methods are trivial, these diagrams show variations of them versus their initial values. Beside, time axis has been scaled in terms of logarithm to help to expose the changes better and clearer.

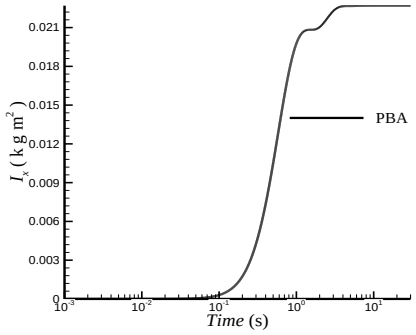

Figure 14. Variations of inertia parameter I_x

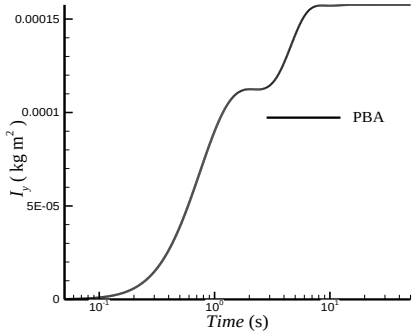

Figure 15. Variations of inertia parameter I_y

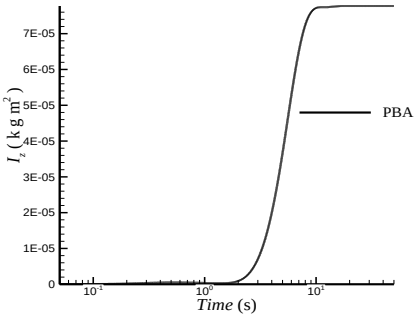

Figure 16. Variations of inertia parameter I_z

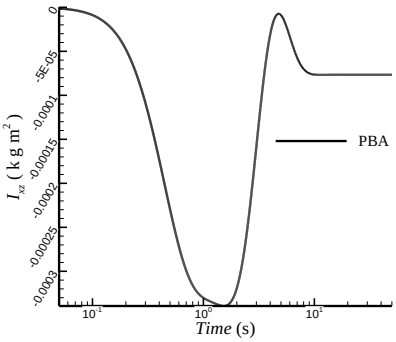

Figure 17. Variations of inertia parameter I_{xz}

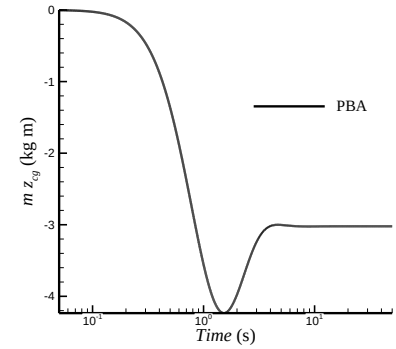

Figure 18. Variations of inertia parameter mz_{cg}

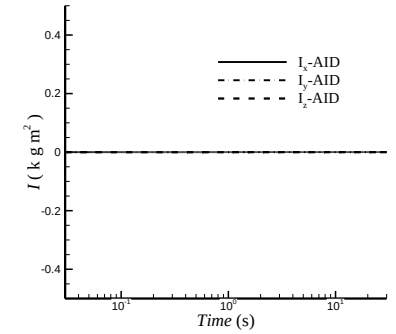

Figure 19. Variations of inertia parameter I_x, I_y, I_z

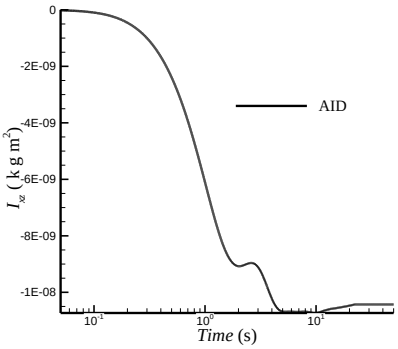

Figure 20. Variations of inertia parameter I_{xz}

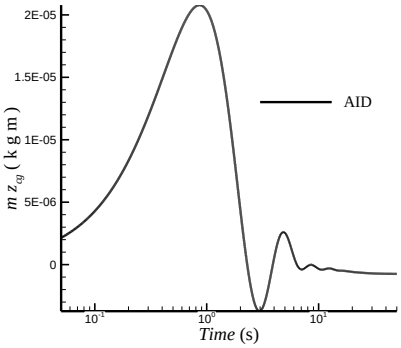

Figure 21. Variations of inertia parameter mz_{cg}

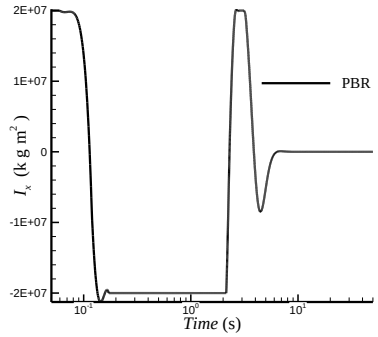

Figure22. Variations of inertia parameter I_x

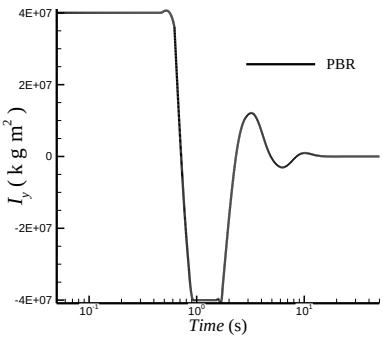

Figure 23. Variations of inertia parameter I_y

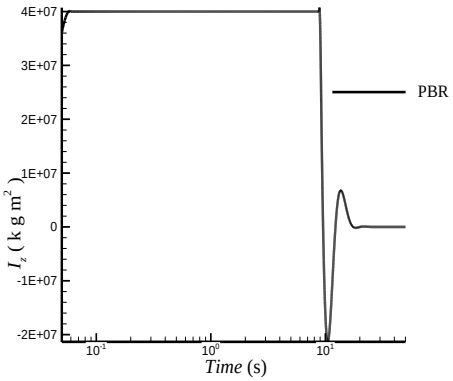

Figure 24. Variations of inertia parameter I_z

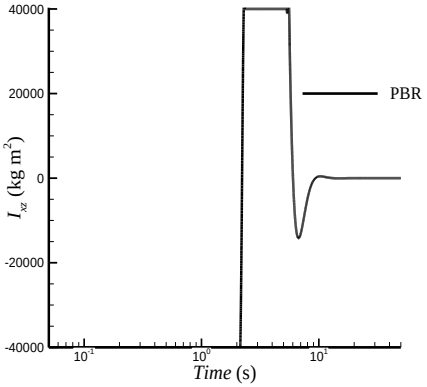

Figure 25. Variations of inertia parameter I_{xz}

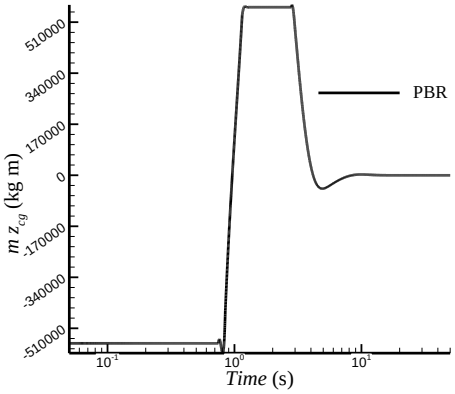

Figure 26. Variations of inertia parameter mz_{cg}

7. Conclusion

In this paper dynamic modeling, adaptive and robust control of an airship model has been addressed. By assuming uncertainties in inertia parameters,simulation results revealed that the closed-loop system is asymptotically stable. This means that asymptotic convergence of tracking the path, after transient state, can be guaranteed for spiral path. Both adaptive and robust control methods, when comparing all three methods, give almost identical results and in comparison with adaptive inverse dynamic have smaller settling time and reach stability faster, respectively, but have more overshoot is a fact.

Also, according to the results concluded from estimating inertia parameters it is clear that all of them are stable in all three methods. In adaptive control based on passivity, parameters are subject to little fluctuations; however, they do not converge to the exact right value. Moreover, in adaptive inverse dynamic method just two of those parameters change, while others remain the same. As it can be seen in [5] and [13], since the inertia parameters have great values the convergence step becomes almost like a forward line, although parameters do not converge to their correct values. Even though in robust control technique parameters converge to their right values in transient state, they return to their initial values in the end.

This should be noted that the methods applied to fully-actuated airship are feasible; nevertheless, under-actuated airships have to be studied much more.

Appendix

Aerodynamic forces and torques are defined as below [6].

Sign content	
B_g	Buoyant force (N)
$F_{T,L}$	Left thrust force (N)
$F_{T,R}$	Right thrust force (N)
g	Gravity acceleration (ms^{-2})
$\{k_1, k_2, k_3\}$	Inertia coefficient
$\{L_a, M_a, N_a\}$	Aerodynamic torques
m	Mass of airship (kg)
Q	Dynamic pressure ($kgm^{-1}s^{-2}$)
u_F, u_δ	Control inputs
v	Linear velocities of the airship (m/s)
$\{X_a, Y_a, Z_a\}$	Aerodynamic forces
$\{x_{cg}, z_{cg}\}$	Coordinates of center of mass (m)
$\{x_p, y_p, z_p\}$	The position of motors (m)
∇	Volume of airship's trunk (m^3)
Greece signs	
γ	Airship's orientation (rad)
$\delta_{ELV}, \delta_{RUD}$	Elevators' and rudders' deviations (rad)
ζ	Airship's position (m)
η	Inertia parameters
μ	Generalized coordinates
μ_L	Left impeller's rotational angle (rad)
μ_R	Right impeller's rotational angle (rad)
ξ	Open angle of left and right motors (rad)
ξ_{diff}	Optimized attenuation coefficient
ρ	Atmosphere density in flight attitude (kgm^{-3})
ρ_i	Constant bound of inertia parameters
ω	Airship's angular velocities (rad/s)
ω_{diff}	Bandwidth (1/s)
Indexes	
c	Desired
cg	Center of mass
d	Desired

References

[1] J.R. Azinheria, A. Moutinho, Paiva, A backstepping controller for path-tracking of an underactuated autonomous airship, International Journal of Robustand Nonlinear Control 19(4) (2010) 418– 441.

[2] G.H. Khoury, J.D. Gillett, Airship technology. First Edittion, Cambridge University Press, 1999.

[3] E. Hygounenc, P. Soueres, Automatic airship control involving backstepping techniques, In Proceedings of the IEEE International Conference on Systems, Man and Cybernetics, Tunisia, October 6– 9 (2002).

[4] J.R. Azinheria, A. Moutinho, Paiva, A backstepping controller for path-tracking of an underactuated autonomous airship, International Journal of Robustand Nonlinear Control, 19(4) (2010) 418– 441.

[5] G.H. Khoury, J.D. Gillett, Airship technology. First Edittion, Cambridge University Press, 1999.

[6] E. Hygounenc, P. Soueres, Automatic airship control involving backstepping techniques, In Proceedings of the IEEE International Conference on Systems, Man and Cybernetics, Tunisia, October 6– 9 (2002).

[7] A. Moutinho, J.R. Azinheria, Stability and robustness analysis of the aurora airship control system using dynamic inversion, In IEEE International Conference on Robotics and Automation(ICRA), Barcelona, Spain, April 18– 22 (2005).

[8] W. Yongmei, Z. Ming, Z. Zongyu, Z. Zewei, Adaptive Trajectory Tracking of Stratospheric Airship Based on Input-output Stability Theory, Computational Intelligence and Design(ISCID), Hangzhou, China, October 28– 30 (2011).

[9] M.W. Spong, S. Hutchinson, M. Vidyasagar, Robot Modeling and Control. First Edittion, John Wiley & Sons, New York, 2006.

[10] M. Alitavoli, M. Taherkhorsandi, M. J. Mahmoodabadi, Ahmad Bagheri, B Miripour-Fard, Pareto design of sliding-mode tracking control of a biped robot with aid of an innovative particle swarm optimization, IEEE International

Symposium on Innovations in Intelligent Systems and Applications (INISTA) (2012).

[11] M. TaherKhorsandi, B. Miripour-Fard, Ahmad Bagheri, Optimal tracking control of a biped robot walking in the lateral plane, IEEE International Symposium on Innovations in Intelligent Systems and Applications (INISTA), (2011).

[12] B. MiripourFard, A. Bagheri, N.Nariman-Zadeh, Limit cycle walker push recovery based on a receding horizon control scheme, Proceedings of the Institution of Mechanical Engineers, Part I: Journal of Systems and Control Engineering 226 (7) (2012) 914– 926.

[13] Z. Zheng, L. Sun, Nonlinear adaptive trajectory tracking control for a stratospheric airship with parametric uncertainty, Nonlinear Dynamics 82(3) (2015) 1416– 1430.

[14] Z. Zheng, W. Hou, Z. Wu, Trajectory tracking Control for underactuated stratospheric airship, Space research 50(7) (2012) 906– 917.

[15] J. B. Mueller, M.A. Paluszek, Y.Y. Zhao, B. Kamkari, Development of an Aerodynamic Model and Control Law Design for a High Altitude Airship, AIAA 3rd, Unmanned Unlimited, Technical Conference, Illinois, September 23 (2004).

[16] B. Zhu, W. Huo, Trajectory Linearization Control for a Quadrotor Helicopter, Control and Automation (ICCA), Xiamen, China, Oct 28– 30 (2011).

[17] M. W. Spong, , On the robust control of robot manipulators, IEEE Transaction on Automatic Control 37(11) (1992) 1782– 1786.